SCIENCE CHINA
Information Sciences

• RESEARCH PAPER •

February 2022, Vol. 65 122404:1–122404:7
https://doi.org/10.1007/s11432-020-3246-8

Spin logic operations based on magnetization switching by asymmetric spin current

Yucai LI[1,2], Nan ZHANG[1,2] & Kaiyou WANG[1,2,3*]

[1]*State Key Laboratory of Superlattices and Microstructures, Institute of Semiconductors, Chinese Academy of Sciences, Beijing* 100083*, China;*
[2]*College of Materials Science and Opto-Electronic Technology, University of Chinese Academy of Sciences, Beijing* 100049*, China;*
[3]*Beijing Academy of Quantum Information Sciences, Beijing* 100193*, China*

Received 20 December 2020/Revised 23 February 2021/Accepted 10 April 2021/Published online 9 November 2021

Abstract Spintronic devices based on spin orbit torques (SOT) exhibit advantages in low power consumption, high speed, reconfigurability, and high endurance, which offers the prospect of in-memory computing based on spin logic devices. By designing a local spin current gradient, the magnetization can be switched deterministically by asymmetric spin currents without external magnetic field using micromagnetic simulations, where an additional out of plane effective field can be generated by the spin gradient. Through capping half of the Pt/Co/Pt SOT devices with Pt strip, we demonstrate the field-free deterministic current-induced magnetization switching experimentally. Finally, we design AND, NAND, OR, and NOR Boolean logic gates based on these devices, which could be used as building blocks for programmable and stateful logic operations.

Keywords spin orbit torque, spin currents, spin current gradient, magnetization switching, spin logic

Citation Li Y C, Zhang N, Wang K Y. Spin logic operations based on magnetization switching by asymmetric spin current. Sci China Inf Sci, 2022, 65(2): 122404, https://doi.org/10.1007/s11432-020-3246-8

1 Introduction

Recently, the rapidly growing demands for low power consumption, in-memory computing, and highly efficient devices have been fueled by an unprecedented surge in information processing, artificial intelligence, portable and energy-aware applications. Spintronic device based on spin torque is one of the best candidates [1, 2]. Currently, the magnetic random access memory (MRAM) based on spin-transfer torque (STT) technology has been commercialized [3], where the spin polarized currents tunnel through the barrier layer, and then transfer the angular momentum to the magnetic free layer, resulting in the magnetization switching [4, 5]. However, the writing speed, power consumption, and endurance of the STT-MRAM still need to be improved. Compared with STT, the spin orbit torque (SOT) could switch the magnetization faster with lower power consumption [6–9]. What is more, the in-plane current induced magnetization switching by SOT does not need to pass through the barrier layer, which can significantly improve the endurance of the device. The typical structure of SOT-induced magnetization switching consists of a strong spin-orbit coupling (SOC) layer and a ferromagnet layer [10–12], where the SOT is induced by spin Hall effect [12, 13] in the SOC layer and/or Rashba effect from the interfacial inversion [10, 11] asymmetry.

Spin logic based on the SOT has expressed the potential in in-memory computing due to the high speed and nonvolatility [14–16]. However, the SOT-induced high-density perpendicular magnetic anisotropy (PMA) ferromagnets switching often needs an in-plane magnetic field to assist [1, 17], which restricts the application of the SOT based devices. There have been many efforts focusing on field-free SOT magnetization switching. For example, taking advantages of ferroelectric substrate [18], lateral wedge oxide [19],

---

[*] Corresponding author (email: kywang@semi.ac.cn)

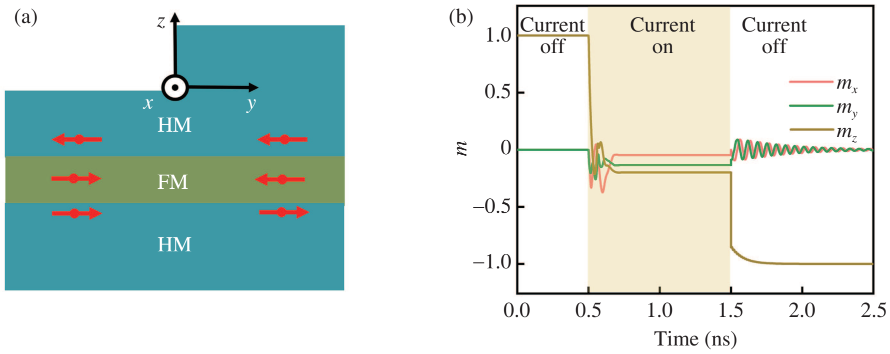

Figure 1 (Color online) Asymmetric spin currents and magnetic dynamic. (a) The schematic of the distribution of the spin currents with different polarizations, (b) the evolution of the magnetization components under the asymmetric spin currents.

exchange coupling between different layers [20], and using lateral SOT [21], current-induced magnetization switching deterministically without magnetic field can be realized. However, the compatibility of the SOT spin logic devices with the commercial fabrication and sophisticated complementary metal oxide semiconductor (CMOS) technology is still needed to be investigated [16].

In traditional SOT structures of heavy metal (HM)/ferromagnet (FM)/HM or HM/FM/insulator stacks, the spin currents generated by the HM layer diffuse into the FM layer. Using micromagnetic simulation, we predicted the rather sharp change of the spin current distribution would induce the deterministic magnetization switching. Accordingly, field-free current-induced magnetization switching in PMA Pt/Co/Pt multilayers was demonstrated with Pt capping half of the areas. The symmetry of spin currents could be tuned to be asymmetry by the Pt capping strip. Based on these devices, we demonstrated different logic operations, which could be utilized as programmable logic gates.

2 Micromagnetic simulations of the asymmetric spin current device

The symmetry of the spin currents could be tuned by changing the thickness of the HM layer in SOT devices. As shown in Figure 1(a), the spin polarization of the spin currents injected from the bottom and top HM layer is the opposite. Depending on the thickness of the HM top layer, the spin polarization of the spin currents injected into the FM layer can change sign and magnitude. On the $+y$ side, the thickness of the top HM layer is larger than that of the bottom layer, and thus the signs of spin polarization and SOT are determined by the top layer. On the other side, the thickness of the bottom HM layer is larger than that of the top layer, the signs of the spin polarization and SOT are opposite to the $+y$ side [21]. And the spin Hall angle of the HM layer could be tuned by the thickness, and thus the magnitude of the spin polarization ratio also is different at two sides [22]. Owing to the asymmetric spin current in these two regions, there will be a transitional region between different spin polarization along the y axis. To simplify, the spin polarization ratio is assumed to vary linearly in the transitional region along the y direction. When the width of Pt is above a certain value (generally reported 3–6 nm), the spin polarization ratio change approaches saturation [22, 23]. So we assume the width of the transitional region is 4 nm to simplify the simulation. The local spin currents gradient in the transitional region could induce an additional effective magnetic field acting on the magnetic layer [18]. Based on the analysis of the spin polarization and the spin currents distribution of the device, the additional current-induced effective magnetic field can be derived as follows: $\boldsymbol{H}_a \approx c\frac{\partial \boldsymbol{J}_s}{\partial y} \approx c\cdot(\frac{\theta_{\mathrm{sh}-y}-\theta_{\mathrm{sh}+y}}{d})\cdot J_e\cdot\hat{\boldsymbol{z}}$, where c is a constant, $\boldsymbol{J}_s$ is the spin current density, J_e is the current density, $\theta_{\mathrm{sh}-y}$ and $\theta_{\mathrm{sh}+y}$ are spin Hall angle at $-y$ side and $+y$ side, and d is width of the transitional region. $\boldsymbol{H}_a$ is proportional to the spin Hall angle difference in the two regions and the current density. The magnetization dynamics could be described by the rewritten Landau-Lifshitz-Gilbert equation:

$$\frac{\partial \boldsymbol{m}}{\partial t} = -\gamma\mu_0\boldsymbol{m}\times\boldsymbol{H}_{\mathrm{eff}} + \alpha\boldsymbol{m}\times\frac{\partial \boldsymbol{m}}{\partial t} + \boldsymbol{\tau}_{\mathrm{DL}} + \boldsymbol{\tau}_{\mathrm{FL}} - \gamma\boldsymbol{m}\times\boldsymbol{H}_a,$$

where $\boldsymbol{m}$ is the unit magnetization vector, $\boldsymbol{H}_{\mathrm{eff}}$ is the effective magnetic field including the magnetic anisotropy field, exchange field, and demagnetization field, α is the Gilbert damping constant, $\boldsymbol{\tau}_{\mathrm{DL}}$

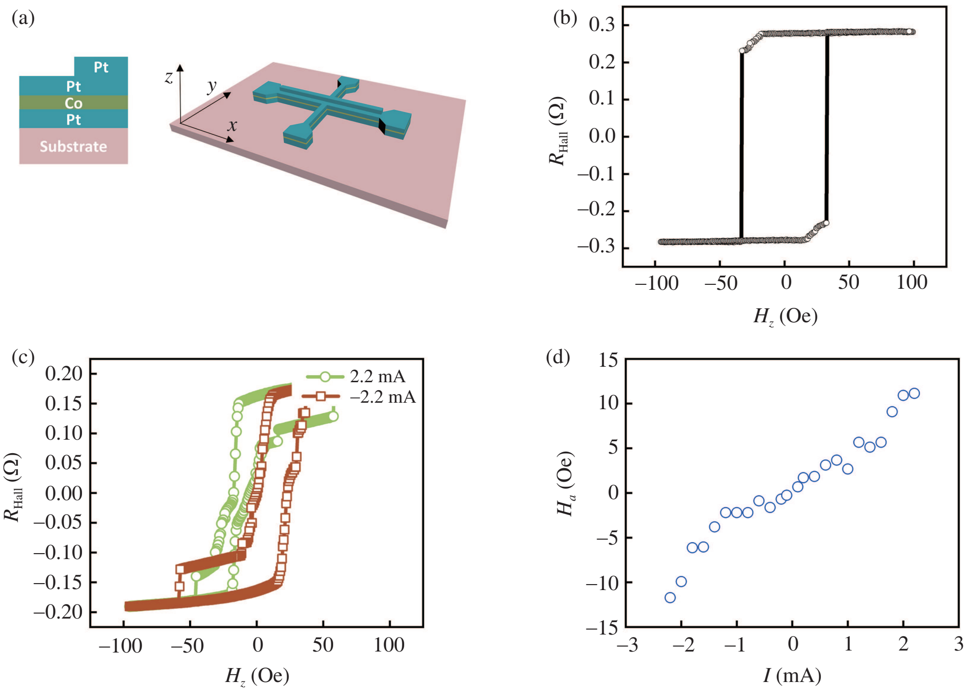

Figure 2 (Color online) Schematic of device structures and the effective field induced by the Pt strip. (a) The structure of the stacks and the device. The Hall bar in the lateral direction is 1 µm wide. (b) Anomalous Hall resistance (offset for clarity) versus out-of-plane magnetic field. (c) Anomalous Hall resistance versus the out-of-plane field with the measuring current of ±2 mA. (d) The effective magnetic field versus d.c. measuring current intensity.

and $\boldsymbol{\tau}_{\rm FL}$ are the damping-like SOT and field-like SOT, respectively [1]. To understand the magnetic dynamics with the asymmetric spin currents, we performed micromagnetic simulations using MuMax3 [24] (material parameters chosen in the simulation were shown in the Supplementary Information). The initial magnetization configuration of the device is set to $m_z = 1$ and relaxed for 0.5 ns before applying current pulse with width $t_p = 1$ ns. Figure 1(b) shows the simulated temporal evolutions of the magnetization components under the asymmetric spin currents. Usually, m_z approaches 0 and m_y approaches ±1 after the current pulse in the traditional HM/FM bilayers structure, which leads to a non-deterministic state if the current is removed [25,26]. However, m_z crosses over 0 under asymmetric spin currents and proceeds to a down state after removing the current, which leads to the deterministic magnetization switching. In Figure 1(b), y components of magnetization at two sides are different, and thus the net magnetization along the y axis does not approach ±1 (snapshots of magnetization profiles are shown in Figure A2).

3 Deterministic current-induced magnetization switching in experiment

To investigate the effective magnetic field induced by the asymmetric spin current, we measured the hysteresis loops under different current intensities in PMA Pt/Co/Pt multilayers. The device structure with stacking arrangement of Pt(3)/Co(0.5)/Pt(2) (thicknesses in nm) is schematically shown in Figure 2(a) (optical microscopy image of the device is shown in Figure B1). The stacks were deposited on Si/SiO2(300 nm) substrate by magnetron sputtering technology. After the stack was processed into 1 µm width Hall bar, a 0.5 µm width stripe pattern was exposed by electron beam lithography. Then the Pt cover strip was fabricated by magnetic sputtering and lift-off technique. The half-covered Pt strip is used to change the distribution of the spin current. The anomalous Hall resistance is measured to check the PMA [27,28]. As shown in Figure 2(b), with sweeping the out-of-plane magnetic field, the square magnetic hysteresis loop was observed, which indicates the good PMA. The hysteresis loop shifts to a negative magnetic field with a current intensity of $I = 2.2$ mA, while it shifts to a positive magnetic field at $I = -2.2$ mA, as shown in Figure 2(c). The effective magnetic field $\boldsymbol{H}_a$ could be extracted from the loop shift: $\boldsymbol{H}_a = -(\boldsymbol{H}_{c-} + \boldsymbol{H}_{c+})/2$, where $\boldsymbol{H}_{c-}$ and $\boldsymbol{H}_{c+}$ are the coercive fields at negative and positive magnetic field, respectively. The function of the effective magnetic field versus direct current

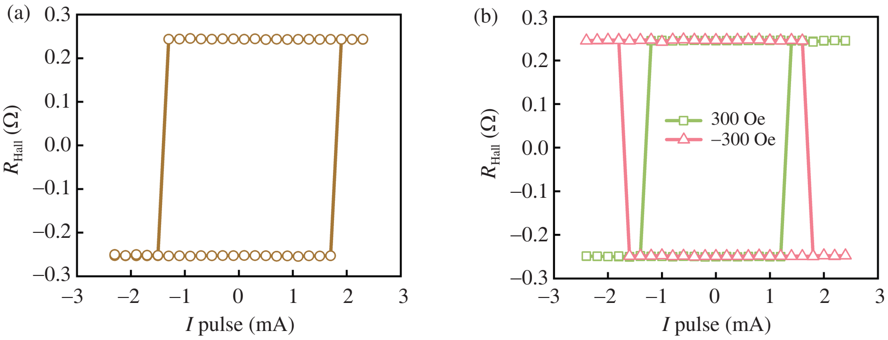

Figure 3 (Color online) Current-induced magnetization switching (a) without external magnetic field and (b) in the presence of ±300 Oe along the current direction.

(d.c.) current intensity is shown in Figure 2(d). By changing the current direction, the effective magnetic field will also change the sign. The magnitude of $\boldsymbol{H}_a$ increases with increasing the current intensity, which is consistent with the effective magnetic field derived from the spin distribution.

To verify the simulation result of the deterministic magnetization switching with the presence of the asymmetric spin current, we measured the current-induced magnetization switching in the absence of the magnetic field by using current pulses. After each pulse, a small current of 100 µm following 5000 ms interval is used to detect the magnetic state avoiding the heating effect. The chirality of the magnetization switching without a magnetic field is determined by the direction of the effective field. As shown in Figure 3(a), the positive effective field induced by positive currents assists magnetization switching from down to up, and the negative effective field induced by negative currents assists magnetization switching from up to down. Current-induced magnetization switching under $H_x = \pm 300$ Oe also was measured, which is shown in Figure 3(b). The magnetization switching loop is anticlockwise under $H_x = 300$ Oe and clockwise under $H_x = -300$ Oe. The opposite H_x results in magnetization switching with different chirality, which is consistent with previous reports [13, 29]. However, it is worth noting that the critical current under $H_x = 300$ Oe is 1.2 mA and the critical current under $H_x = -300$ Oe is 1.6 mA. It suggests the effective magnetic field induced by the Pt strip has an influence on the critical current [30]. Under $H_x = 300$ Oe, the positive currents switch magnetization from down to up, the positive effective field favors magnetization switching, and thus the critical current is reduced. However, under $H_x = -300$ Oe, the positive currents switch magnetization from up to down, and the positive effective field hinders the magnetization switching, which will increase the critical current. With negative current, the negative effective field also could decrease the critical current under $H_x = 300$ Oe and increase the critical current under $H_x = -300$ Oe.

Pt strip can not only generate local spin current gradient by changing the magnitude of the spin currents, but also change the sign of the spin polarization. The effective thickness of the Pt layer that could generate net spin current is the thickness of the top Pt layer minus the bottom Pt layer [21]. To simplify, assuming the spin current density is proportional to the effective thickness of the Pt layer, we then can separate these two effects by designing devices with different thicknesses of the Pt layers. As shown in Figure 4(a) and (b), the two devices have the same spin current gradient owing to the same effective thickness difference between the top and bottom Pt layer at two sides. However, the sign of the spin polarization is the same for Figure 4(a) while opposite for Figure 4(b) for the two regions. Alternative positive and negative current pulses above switching critical current were applied to devices in the absence of magnetic field, a small current of 100 µA following 5000 ms interval was used to detect the magnetic state after each pulse. As shown in Figure 4(a) and (b), deterministic magnetization switching behaviors were observed in devices with different Pt thicknesses, which means that the local spin currents gradient generated by the Pt strip dominates the magnetization switching.

4 Logic operations based on the devices

Based on the devices, we demonstrated the four common Boolean logic gates AND, NAND, OR, and NOR. Figure 5(a) shows the truth table of these logic operations. The AND (OR) and NAND (NOR) are complementary function pairs, whose outputs are always contrary. Devices with opposite switching

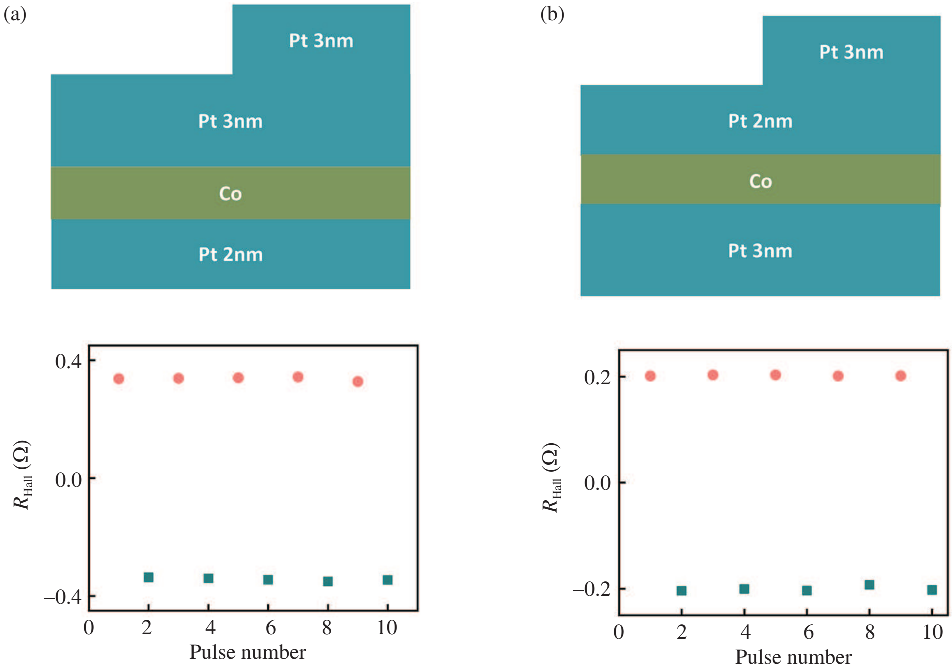

Figure 4 (Color online) Magnetization switching with alternative positive and negative in-plane currents. (a) Magnetization switching in Pt(2 nm)/Co(0.5 nm)/Pt(3 nm)/Pt strip (3 nm). (b) Magnetization switching in Pt(3 nm)/Co(0.5 nm)/Pt(2 nm)/Pt strip (3 nm).

chirality are used to demonstrate the complementary functions. The switching chirality depends on the position of the Pt strip, which is shown in Figure 5(b) and (c). The inputs and outputs of the logic gates are shown in Figure 5(d)–(i). The reset current $I_{\rm ret} = \pm 2$ mA is used to reset the magnetization state before logic operation. Two applied currents I_A and I_B are functioning as two inputs, both of them are 1 and −1 mA for inputs "1" and "0". In this way, the actually applied current is one of three kinds of overlapped current pulses $I_{\rm ovlp} = -2, 0, 2$ mA. The magnetization up state is defined as output "1" while the magnetization down state is defined as output "0". The Pt strip on $+y$ was used to demonstrate the "AND" and "OR" gates. For the "AND" gate, the magnetization is set to down state by applying the reset current of −2 mA. When $A = 1$, $B = 0$ and $A = 0$, $B = 1$, the overlapped current pulses $I_{\rm ovlp}$ are 0, and then the outputs are depended on the reset current. When $A = B = 0$, the overlapped current pulses $I_{\rm ovlp}$ are −2 mA, which could not change the state of the magnetization, the outputs are 0. Only when $A = B = 1$, the overlapped current pulses $I_{\rm ovlp}$ are 2 mA, the magnetization could be switched from down to up state, the outputs are 1. For the "OR" gate, the magnetization is set to be up state by applying the reset current of 2 mA. Only when $A = B = 0$, the overlapped current pulses $I_{\rm ovlp} = -2$ mA could switch the magnetization from up to down state, the outputs is 0. The Pt strip on $-y$ was used to demonstrate the "NAND" and "NOR" gate. For the "NAND" gate, the magnetization is set to be up state by applying the reset current of −2 mA. Only when $A = B = 1$, the overlapped current pulses $I_{\rm ovlp} = 2$ mA could switch the magnetization from up to down state, the outputs are 0. For the "NOR" gate, the magnetization is set to be down state by applying the reset current of 2 mA. Only when $A = B = 0$, the overlapped current pulses $I_{\rm ovlp} = -2$ mA could switch the magnetization from down to up state, the outputs are 1. These logic gates could be used as building blocks for programmable and stateful logic operations [31]. For application, we propose a kind of MTJ, which could be integrated into our structure.

5 Conclusion

In summary, we have demonstrated the magnetization switching induced by asymmetric spin currents. The spin currents are tuned by the Pt strip deposited on the Pt/Co/Pt devices. As proposed in micromagnetic simulations, the out-of-plane effective field induced by the local spin current gradient can assist deterministic current-induced magnetization switching in the absence of a magnetization field. Spin

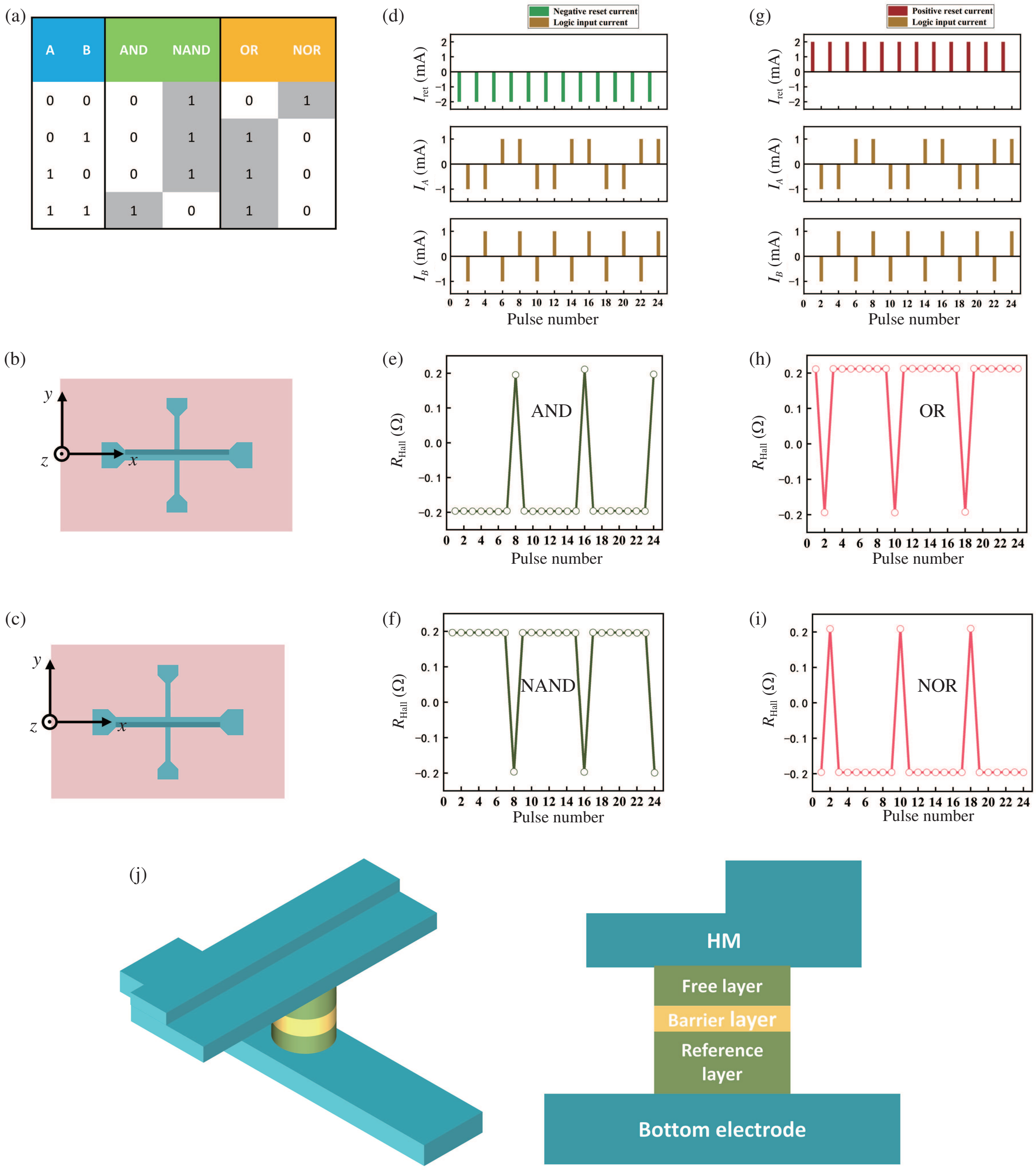

A	B	AND	NAND	OR	NOR
0	0	0	1	0	1
0	1	0	1	1	0
1	0	0	1	1	0
1	1	1	0	1	0

Figure 5 (Color online) Initialization of current-programmable Boolean logic operating on the complementary spin logic device and schematic illustration of the MTJ. (a) Truth tables of AND, NAND, OR, and NOR Boolean logic gates. (b) and (c) Schematic drawings of devices with Pt capping layer at different sides. (d)–(i) Demonstration of initialization current-programmable Boolean logic gates using the above two devices. Binary logic inputs of two current pulses I_A and I_B ($-1/+1$ mA stands for logic value "0"/"1") were applied along the Hall bar channel simultaneously. The resulting nonvolatile current-induced magnetization down/up state is regarded as logic output value "0"/"1". The x-axes of (d)–(i) are operation procedures with the same scales and values. (j) Schematic illustration of the SOT based MTJ structure.

logic operations based on asymmetric spin currents devices provide a new way to achieve programmable and stateful logic operations. Our study could be important for developing future in-memory computing spintronic devices.

Acknowledgements This work was supported by Beijing Natural Science Foundation Key Program (Grant No. Z190007), National Natural Science Foundation of China (Grant Nos. 61774144, 12004376), Key Research Program of Frontier Sciences, CAS (Grant No. QYZDY-SSW-JSC020), and the Strategic Priority Research Program of the Chinese Academy of Sciences (Grant Nos. XDB28000000, XDB44000000).

Supporting information Appendixes A and B. The supporting information is available online at info.scichina.com and link.springer.com. The supporting materials are published as submitted, without typesetting or editing. The responsibility for scientific accuracy and content remains entirely with the authors.

References

1 Li Y, Edmonds K W, Liu X, et al. Manipulation of magnetization by spin-orbit torque. Adv Quantum Technol, 2019, 2: 1800052

2 Khvalkovskiy A V, Apalkov D, Watts S, et al. Basic principles of STT-MRAM cell operation in memory arrays. J Phys D-Appl Phys, 2013, 46: 074001

3 Aggarwal S, Almasi H, DeHerrera M, et al. Demonstration of a reliable 1 Gb standalone spin-transfer torque MRAM for industrial applications. In: Proceedings of IEEE International Electron Devices Meeting (IEDM), 2019. 1–4

4 Slonczewski J C. Current-driven excitation of magnetic multilayers. J Magn Magn Mater, 1996, 159: 1–7

5 Berger L. Emission of spin waves by a magnetic multilayer traversed by a current. Phys Rev B, 1996, 54: 9353–9358

6 Bhatti S, Sbiaa R, Hirohata A, et al. Spintronics based random access memory: a review. Mater Today, 2017, 20: 530–548

7 Jabeur K, Di Pendina G, Bernard-Granger F, et al. Spin orbit torque non-volatile flip-flop for high speed and low energy applications. IEEE Electron Device Lett, 2014, 35: 408–410

8 Prenat G, Jabeur K, Vanhauwaert P, et al. Ultra-fast and high-reliability SOT-MRAM: from cache replacement to normally-off computing. IEEE Trans Multi-Scale Comp Syst, 2016, 2: 49–60

9 Zhang N, Zhang B, Yang M-Y, et al. Progress of electrical control magnetization reversal and domain wall motion (in Chinese). Acta Phys Sin, 2017, 66: 027501

10 Miron I M, Gaudin G, Auffret S, et al. Current-driven spin torque induced by the Rashba effect in a ferromagnetic metal layer. Nat Mater, 2010, 9: 230–234

11 Miron I M, Garello K, Gaudin G, et al. Perpendicular switching of a single ferromagnetic layer induced by in-plane current injection. Nature, 2011, 476: 189–193

12 Liu L, Pai C F, Li Y, et al. Spin-torque switching with the giant spin Hall effect of tantalum. Science, 2012, 336: 555–558

13 Liu L, Lee O J, Gudmundsen T J, et al. Current-induced switching of perpendicularly magnetized magnetic layers using spin torque from the spin Hall effect. Phys Rev Lett, 2012, 109: 096602

14 Parveen F, Angizi S, He Z, et al. Low power in-memory computing based on dual-mode SOT-MRAM. In: Proceedings of IEEE/ACM International Symposium on Low Power Electronics and Design (ISLPED), 2017. 1–6

15 Baek S C, Park K W, Kil D S, et al. Complementary logic operation based on electric-field controlled spin-orbit torques. Nat Electron, 2018, 1: 398–403

16 Wang X, Wan C, Kong W, et al. Field-free programmable spin logics via chirality-reversible spin-orbit torque switching. Adv Mater, 2018, 30: 1801318

17 Yang M, Cai K, Ju H, et al. Spin-orbit torque in Pt/CoNiCo/Pt symmetric devices. Sci Rep, 2016, 6: 20778

18 Cai K, Yang M, Ju H, et al. Electric field control of deterministic current-induced magnetization switching in a hybrid ferromagnetic/ferroelectric structure. Nat Mater, 2017, 16: 712–716

19 Yu G, Upadhyaya P, Fan Y, et al. Switching of perpendicular magnetization by spin-orbit torques in the absence of external magnetic fields. Nat Nanotech, 2014, 9: 548–554

20 Sheng Y, Edmonds K W, Ma X, et al. Adjustable current-induced magnetization switching utilizing interlayer exchange coupling. Adv Electron Mater, 2018, 4: 1800224

21 Cao Y, Sheng Y, Edmonds K W, et al. Deterministic magnetization switching using lateral spin-orbit torque. Adv Mater, 2020, 32: 1907929

22 Ganguly A, Kondou K, Sukegawa H, et al. Thickness dependence of spin torque ferromagnetic resonance in $Co_{75}Fe_{25}$/Pt bilayer films. Appl Phys Lett, 2014, 104: 072405

23 Li S H, Lim G J, Gan W L, et al. Tuning the spin-orbit torque effective fields by varying Pt insertion layer thickness in perpendicularly magnetized Pt/Co/Pt(t)/Ta structures. J Magn Magn Mater, 2019, 473: 394–398

24 Vansteenkiste A, Leliaert J, Dvornik M, et al. The design and verification of MuMax3. AIP Adv, 2014, 4: 107133

25 Chen B J, Lourembam J, Goolaup S, et al. Field-free spin-orbit torque switching of a perpendicular ferromagnet with Dzyaloshinskii-Moriya interaction. Appl Phys Lett, 2019, 114: 022401

26 Yan S, Bazaliy Y B. Phase diagram and optimal switching induced by spin Hall effect in a perpendicular magnetic layer. Phys Rev B, 2015, 91: 214424

27 Karplus R, Luttinger J M. Hall effect in ferromagnetics. Phys Rev, 1954, 95: 1154–1160

28 Sinova J, Valenzuela S O, Wunderlich J, et al. Spin Hall effects. Rev Mod Phys, 2015, 87: 1213–1260

29 Li Y, Liang J, Yang H, et al. Current-induced out-of-plane effective magnetic field in antiferromagnet/heavy metal/ferromagnet/heavy metal multilayer. Appl Phys Lett, 2020, 117: 092404

30 Lee J M, Cai K, Yang G, et al. Field-free spin-orbit torque switching from geometrical domain-wall pinning. Nano Lett, 2018, 18: 4669–4674

31 Zhang N, Cao Y, Li Y, et al. Complementary lateral-spin-orbit building blocks for programmable logic and in-memory computing. Adv Electron Mater, 2020, 6: 2000296